Communication via gap junctions underlies early functional and beneficial interactions between grafted neural stem cells and the host

Johan Jäderstad[a,1], Linda M. Jäderstad[a,1], Jianxue Li[b,2], Satyan Chintawar[c,2], Carmen Salto[d], Massimo Pandolfo[c], Vaclav Ourednik[b], Yang D. Teng[e], Richard L. Sidman[b,3], Ernest Arenas[d], Evan Y. Snyder[b,f,3], and Eric Herlenius[a,3]

[a]Department of Women's and Children's Health and; [d]Department of Medical Biochemistry and Biophysics, Karolinska Institutet, 17176 Stockholm, Sweden; [b]Department of Neurology, Beth Israel Deaconess Medical Center, Boston, MA 02215; [c]Service de Neurologie, Hôpital Erasme–University Libre de Bruxelles, 1070 Brussels, Belgium; [e]Department of Neurosurgery, Brigham & Women's Hospital, Boston, MA 02215; and [f]Burnham Institute for Medical Research, La Jolla, CA 92037

Contributed by Richard L. Sidman, January 5, 2010 (sent for review November 25, 2009)

How grafted neural stem cells (NSCs) and their progeny integrate into recipient brain tissue and functionally interact with host cells is as yet unanswered. We report that, in organotypic slice cultures analyzed by ratiometric time-lapse calcium imaging, current-clamp recordings, and dye-coupling methods, an early and essential way in which grafted murine or human NSCs integrate functionally into host neural circuitry and affect host cells is via gap-junctional coupling, even before electrophysiologically mature neuronal differentiation. The gap junctions, which are established rapidly, permit exogenous NSCs to influence directly host network activity, including synchronized calcium transients with host cells in fluctuating networks. The exogenous NSCs also protect host neurons from death and reduce such signs of secondary injury as reactive astrogliosis. To determine whether gap junctions between NSCs and host cells may also mediate neuroprotection in vivo, we examined NSC transplantation in two murine models characterized by degeneration of the same cell type (Purkinje neurons) from different etiologies, namely, the *nervous* and *SCA1* mutants. In both, gap junctions (containing connexin 43) formed between NSCs and host cells at risk, and were associated with rescue of neurons and behavior (when implantation was performed before overt neuron loss). Both in vitro and in vivo beneficial NSC effects were abrogated when gap junction formation or function was suppressed by pharmacologic and/or RNA-inhibition strategies, supporting the pivotal mediation by gap-junctional coupling of some modulatory, homeostatic, and protective actions on host systems as well as establishing a template for the subsequent development of electrochemical synaptic intercellular communication.

Reestablishment of functional networks in the central nervous system (CNS) has been proffered as one of the goals of stem cell–mediated therapeutics. Although this is clearly one strategy, it may not be the easiest, or even the most likely basis for the beneficial outcomes in most reported cases of recovery to date. The number of neural stem cells (NSCs), for example, that differentiate into mature well-integrated neurons, and the lengthy time this process requires, are usually insufficient to account for the improvement. Although it is becoming recognized that grafted NSCs interact with—indeed, sustain, rescue, or protect—endogenous imperiled neurons in vivo (1–3), the underlying mechanisms are poorly characterized. Although, in some cases, we and others have attributed this action to the release of diffusible cytokines from NSCs (1, 2), this mechanism alone is inadequate for explaining all cases (3). A better understanding of the iterative developmental process by which grafted NSCs integrate into host neural tissue may provide insights into the interplay between donor and host. Here we report that an early and essential step in the functional integration of grafted murine and human NSCs into host neural circuitry, even before (and perhaps establishing a template for) mature electrochemical synaptic communication, is cell–cell coupling via gap junctions that modulate network activity. When we observed that such gap junction formation also seemed to inhibit death of host neurons and suppress such inimical processes as gliosis, we further hypothesized that this mode of direct intercellular communication between exogenous NSCs and host cells might constitute an underappreciated mechanism by which stem cells exert a homeostatic and/or protective effect on endangered host cells. Indeed, these therapeutic actions by NSCs could be abrogated by blocking gap junction formation or function. That such gap junctions may mediate translationally relevant neuroprotection was suggested by observing their role in the NSC-mediated rescue of host neurons and their projections in representative models of neurodegeneration—effects noted only when direct cell–cell contact via functional gap junctions were made.

Results

Differentiation and Integration of Grafted NSCs. To examine the stages of exogenous NSC integration into host neural cytoarchitecture, we initially used a rodent striatal organotypic slice culture system (4) into which were grafted early passages of a stable clonal population of murine NSCs (mNSCs) (5). To track and record from individual cells in situ, a subclone was engineered to overexpress green fluorescent protein (GFP). Grafted mNSCs migrated throughout the organotypic cultures (OCs) (Fig. 1, Fig. S1, and Movie S1). Whereas at 7 days postimplantation, ~25% expressed nestin (a marker of the undifferentiated state) (Fig. S1) and ~20% expressed glial fibrillary acidic protein (GFAP), an intermediate filament protein and an astroglial and progenitor cell marker (Fig. S1), by 28 days in vivo (DIV), few mNSC-derived cells were nestin+ (0.1%) or GFAP+ (0.6%) (Fig. S1 and Table S1). Expression of the early neuronal marker β-III tubulin (Tuj1) increased in these mNSCs from 39% (7 DIV) to 71% (28 DIV) (Fig. S1 and Table S1 and expression of the more mature neuronal marker MAP2ab increased from $4 \pm 1\%$ (7 DIV) to $19 \pm 4\%$ (28 DIV). Of endogenous cells in the OCs, ~40% were Tuj1+ throughout the culture period (Fig. S1) and showed no change in resting membrane potential (V_m) or membrane resistance (R_m) over that time span. Grafted mNSCs, by contrast, displayed significant developmental differences in both V_m and R_m (Fig. S2). Although unengrafted mNSCs ($n = 10$) displayed no active membrane properties (Na^+/K^+ channel activity), by 28 DIV, 66% of mNSCs did ($n = 32$), indicative of differentiation toward a neuronal

Author contributions: J.J., V.O., R.L.S., E.Y.S., and E.H. designed research; J.J., L.M.J., J.L., S.C., C.S., Y.D.T., and E.H. performed research; M.P., R.L.S., E.Y.S., and E.H. contributed new reagents/analytic tools; J.J., L.M.J., J.L., S.C., C.S., M.P., V.O., Y.D.T., R.L.S., E.A., E.Y.S., and E.H. analyzed data; and J.J., R.L.S., E.Y.S., and E.H. wrote the paper.

The authors declare no conflict of interest.

Freely available online through the PNAS open access option.

[1]J.J. and L.M.J. contributed equally to this work.

[2]J.L. and S.C. contributed equally to this work.

[3]To whom correspondence may be addressed. E-mail: Eric.Herlenius@ki.se, esnyder@burnham.org, or richard_sidman@hms.harvard.edu.

This article contains supporting information online at www.pnas.org/cgi/content/full/0915134107/DCSupplemental.

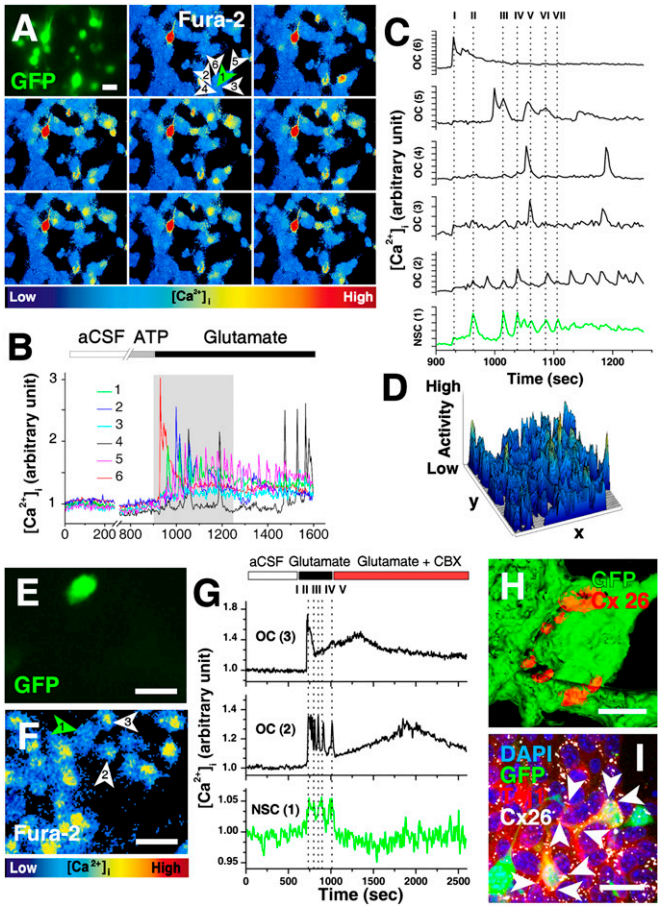

Fig. 1. Grafted mNSC and host cell interactions in fluctuating networks are blocked by inhibiting gap junction function. (*A*) Communication between grafted mNSCs (GFP+, green arrowhead) and endogenous OC cells tracked by ratiometric $[Ca^{2+}]_i$ imaging. (*B*) Typical $[Ca^{2+}]_i$ response, after 14 DIV, of mNSC (no. 1) and endogenous OC cells (nos. 2–6) in *A*. Note that no spontaneous $[Ca^{2+}]_i$ events are detected during control conditions (aCSF) or during ATP application. Glutamate causes an instantaneous rise in $[Ca^{2+}]_i$ and induces temporary coupled oscillations in both mNSCs and OC cells. $[Ca^{2+}]_i$ traces (gray box in *B*) are enlarged in *C*. The mNSC trace is green; overlapping events are marked with dotted lines *I–VII*. (*D*) Activity plot showing even variations in Ca^{2+} transients in all parts of the field (Movie S3). (*E* and *F*) mNSC (green cells in *E* and green arrowhead in *F*) and OC cells (white arrowheads in *F*) characterized by time lapse $[Ca^{2+}]_i$ imaging (*F*). Curves in *G* depict the $[Ca^{2+}]_i$ response of cells 1–3 in *F*. Overlapping events are marked with dotted lines *I–V*. Glutamate causes an instantaneous rise in $[Ca^{2+}]_i$ and induced temporary coupled oscillations in both mNSCs and OC cells. Addition of gap junction inhibitor CBX disrupts the synchronous communication and uncouples the successive low frequency fluctuations. (*H* and *I*) Intercellular gap-junctional contacts (here Cx26) between GFP+ (green) mNSCs themselves (red punctate immunopositivity in *H*); between mNSCs and OC cells; and between host OC cells themselves (white punctate immunopositivity in *I*) (Movie S4). White arrows in *I* mark gap-junctional plaques between Tuj1+ mNSC-derived cells and OC cells. (Bars: 20 μm, *A, E, F,* and *I;* 5 μm, *H*).

phenotype. However, even after 28 DIV, the number of Na^+/K^+ channels in the neuronal mNSC progeny was insufficient to generate repetitive action potentials like those characteristic of completely mature neurons, suggesting that full neuronal maturation of grafted mNSCs requires longer than 1 month. Furthermore, after 1 month in culture, none of the mNSCs expressed synaptotagmin (indicative of fast Ca^{2+}-dependent synaptic vesicle exocytosis and neurotransmitter release), and postsynaptic potentials (indicative of synaptic input) were detected in <5% of mNSCs.

Despite this evidence of insufficiently mature neuronal differentiation, mNSCs were able to integrate functionally into Ca^{2+}-mediated host networks. Spontaneous $[Ca^{2+}]_i$ fluctuations were commonly seen both in grafted (n = 91) and nongrafted (n = 36) OCs (Fig. S2 and Movie S2), and application of ATP or glutamate elicited responses from both (Table S2). Ratiometric Fura-2 $[Ca^{2+}]_I$ imaging showed that grafted mNSCs had integrated in fluctuating functional networks (Fig. 1 *A–G*, Fig. S2 *I–K*, and Movie S3). Ca^{2+}waves propagated between cells at 24 ± 4 μm/s. Fluorescence peak analysis revealed temporal overlaps between mNSCs and neighboring host cells in 50% of OCs, suggesting that mNSC and endogenous OC neural activity were yoked. Application of ATP evoked transient or sustained responses in several, but not all, of the OCs cells and mNSCs (Fig. 1 *A–D* and Movie S3). However, the P2-purinergic receptor antagonist suramin (100 μM) did not affect the synchronized Ca^{2+}waves detected between grafted mNSCs and host cells (investigated in 17 grafted NSC-host cell pairs in four different OCs at 14 DIV), suggesting that these waves and the interplay between OC cell and NSCs were not dependent on ATP-purinergic receptors.

Grafted NSCs Establish Functional Gap Junctions with OC Cells. As the influence of mNSCs on Ca^{2+} waves greatly preceded development of mature neuronal properties and reciprocal electrochemical transynaptic signaling, some antecedent mechanism must have allowed earlier intercellular communication. We postulated that this mechanism might involve formation of gap junctions (6–8). Located on the plasma membrane and composed of connexin (Cx) proteins, gap junctions are clusters of channels connecting the interiors of coupled cells through which molecules <1 kDa may be exchanged. Therefore, we examined expression of Cxs in NSCs and OCs, focusing on Cx26 (Fig. 1 *H–I*) and Cx43 (Fig. 2 and Fig. S2 *L*), Cxs prevalent during neural development (6–11).

Before grafting, ~50% of mNSCs expressed Cx43 and <10% expressed Cx26 (Fig. S3). Within 3 days of grafting, the proportion of mNSCs expressing Cx43 increased to 92 ± 1% (n = 60 OCs) (Fig. 2*A* and *B*) and Cx26 to 24 ± 2% (Fig. 1 *H–I*) (n = 29 OCs). As early as 2–18 h after grafting, mNSCs started to form functional gap junctions with host cells via Cx43 (Fig. 2 *D–L* and Fig. S4). Interestingly, Cx expression in grafted mNSCs appeared to have a developmental dynamic that paralleled that of the maturing cell type identities of mNSC derivatives in the OCs. For example, when most of the NSC-derived cells (70 ± 2%; n = 214) were still at a NSC stage (nestin+), the majority of them were Cx43+ (92 ± 1%). Instead, by 7 DIV, when only 25% of the mNSC-derived cells were nestin+ and nearly 40% had become Tuj1+, Cx43 expression decreased to 35% of the mNSC-derived cells (n = 75) (Fig. 2 *A* and Table S1). By 28 DIV, when the mNSCs had predominantly begun to assume a neuronal phenotype, <5% (n = 44) of donor mNSC progeny expressed Cx43 (Fig. 2 and Movie 5) (although all surrounding host astrocytes did so; n = 62). Cx43 was commonly seen in host striatal OCs cells and colocalized with nestin or GFAP. Whereas Cx43 appeared to be most closely associated with immature NSCs and/or non-neuronal cells, Cx26, by contrast, appeared to be most closely associated with neuronally differentiated mNSCs, their predominant fate by 28 DIV (Fig. 1 *H–I*): 98 ± 2% of mNSC-derived Tuj1+ cells (n = 54) and 96 ± 4% of host-derived Tuj1+ cells (n = 177) coexpressed Cx26. Cx26-containing gap junctions were observed between grafted mNSC and host neurons (n = 48), as well as between grafted mNSC themselves (n = 51) and between host neurons themselves (n = 189) (Fig. S1 and Movie S4). Hence, while Cx43 was prominent in the "early" stages of the engrafted OCs' "development" and decreased with time, Cx26 expression increased.

The observations described above for murine NSCs applied as well to bFGF-propagated fetal human NSCs (hNSCs), i.e., NSCs from a different species, expanded and maintained under different conditions. hNSCs also expressed Cx43 upon initial contact with OC cells (Fig. 2 *C* and Movie S8), exhibited functional intercellular communication, and demonstrated a similar pattern of spontaneous and inducible Ca^{2+} flux (Fig. 2 *G* and *H*, Fig. S4,

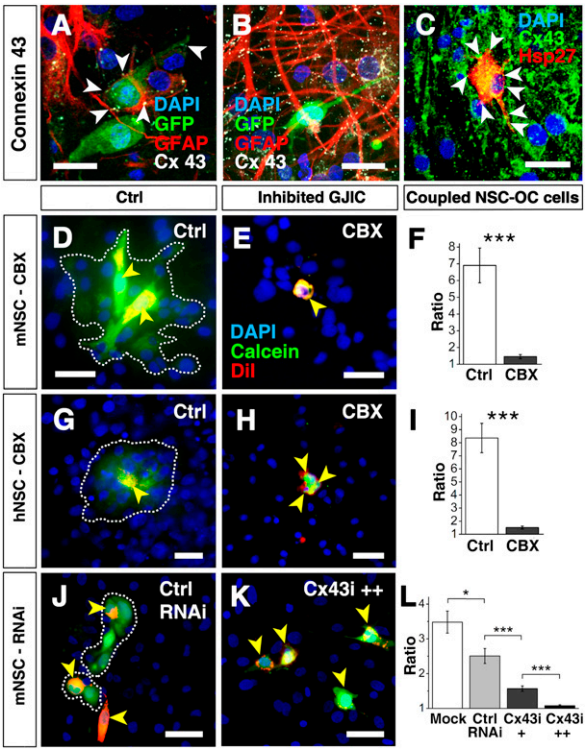

Fig. 2. Gap-junctional couplings between OC cells and murine and human NSCs. (*A* and *B*) Cx43 gap-junctional coupling between GFP+ mNSCs and OC cells is detectable as white punctate immunopositivity (arrowheads) at 7 DIV (*A*) but decreases with time in culture. By 28 DIV (*B*), few of the grafted cells but all of the surrounding astrocytes express Cx43. (*C*) hNSCs (Hsp27) (red), integrate throughout the OC. Cx43 immunopositivity (green) marks gap-junctional plaques between hNSCs and host cells. mNSCs (*D, E, J,* and *K*) and hNSCs (*G* and *H*) (yellow arrowheads), preloaded with the gap junction permeable dye *calcein* (green) and the membrane-bound dye *DiI* (red), integrate and establish functional gap junction connections to OC cells within 4 h after engraftment, indicated by the transfer of the cytosolic calcein dye to juxtaposed DiI-negative host striatal cells, turning them green (white encircled area). (*F* and *I*) The greater the ratio of calcein+ host:donor cells, the greater the degree of dye transfer through functional gap junctions. Transfer is blocked by gap junction inhibitor CBX. (*J–L*) Although mNSCs transfected with control RNAi establish functional intercellular channels within 4 h after engraftment (*J*), transfection with Cx43-RNAi inhibits the formation of functional communication between grafted and host cells in a dose dependent manner (*K*), quantified in *L*. DAPI marks all nuclei blue. $*P < 0.05$; $**P < 0.01$. (Bars: 20 μm.)

and Movie S6 and S7). Ca^{2+} waves propagated between cells at 30 ± 6 μm/s (n = 6 OCs), comparable to that observed in OC.

To confirm that gap junctions established between grafted and host cells were functional, standard dye transfer studies were performed (detailed in *SI Text*). Briefly, donor mNSCs or hNSCs were loaded with gap junction–permeant dyes (e.g., calcein or lucifer yellow), transfer of which to host OC cells was first documented and then suppressed by thepharmacologic gap junction blocking agents carbenoxolone (CBX; 100 μM) or 18-α-glycyrrhetinic acid (C18-α-GA; 50 μM) (Fig. 2 *D–I* and Fig. S4). Pharmacological inhibition of gap junctions not only blocked dye transfer from murine and human NSCs to host cells in vitro (Fig. 2 *D–I* and Fig. S4 *G–L*) but also inhibited coupled Ca^{2+} transients (Fig. 1 *E–G*, Fig. S4 *D–F*, and Movie S7), suggesting that gap-junctional coupling was integral to early intercellular cross-talk and coordination.

Donor NSCs Improve Host Cell Health in OCs via Gap Junction Formation and Function. Although slice cultures are essential for electrophysiological assessments of network functions, it is known that preparation of OCs is a traumatic perturbation involving axotomy with consequent cell death, reactive astrogliosis, and scarring—undesirable but necessary and accepted "collateral damage" (4). Unexpectedly, we observed that, in OCs in which donor NSCs had become integrated via gap junction formation, the baseline proportion of host OC cell death was reduced by 74% compared with OCs without grafted NSCs (0.58 ± 0.67% vs. 2.27 ± 0.58% in nongrafted OCs, n = 42 and 41 respectively, P = 0.005) (Fig. 3 *A–C*). Accordingly, after 72 h, the overall survival of OCs grafted with mNSCs (n = 76) was significantly higher (P = 0.03) compared with control cultures (n = 72). Similarly, high GFAP expression in host cells, conventionally used to monitor the degree of astroglial reaction to the mechanical trauma of establishing the slice, was reduced in grafted slices at 7 and 14 DIV (P = 0.004 and P = 0.008, respectively) (Fig. 3 *D–F* and Fig. S1 *D–F*).

Pharmacological inhibition of gap junction function abrogated the beneficial impact of murine or human NSCs on host cells. For example, the proportion of GFAP+ host cells was 30 ± 6% following hNSC engraftment (n = 8 OCs), but rose nearly 2-fold to 51 ± 4%, the degree of astroglial reaction seen in nongrafted OCs (Fig. 3 *D–F* and Fig. S1*F*), if CBX (50 μM) was applied during the first 3 days postengraftment.

To control for off-target actions of the pharmacologic inhibitors, we complemented these gap junction function-blocking studies by suppressing gap junction formation through silencing Cx26 and Cx43 in mNSCs via RNA interference (RNAi) (Fig. 3 *G–L*, Fig. S5, and *SI Text*). We first established an optimal level of RNAi such that mNSC viability was not compromised, yet Cx expression at both the message and protein levels (as assessed by RT-PCR and Western analysis, respectively) was adequately suppressed for at least 7 DIV. We next affirmed that transducing RNAi constructs into the mNSCs under these conditions did not alter their cell numbers or differentiation profile compared with mock or control-RNAi–transfected NSCs ("Mock" and "Ctrl-RNAi", respectively). Inhibition of Cx43 ranging from 30% to 70% blocked mNSC-mediated beneficial actions (e.g., the antigliotic actions) in a dose-dependent manner. Interestingly, Cx26 suppression alone had little impact on blunting this mNSC action (Fig. 3I and Fig. S5*D*), suggesting that NSCs' therapeutic actions are principally mediated by the developmentally earlier Cx43.

Contact-Dependent Rescue of Neurons by NSCs in Vivo Is Accompanied by and Dependent on Gap Junctions. To explore whether such gap junction–mediated beneficial NSC-host cross-talk might occur in vivo and, hence, hold translational-relevance, we examined the interactions between engrafted NSCs and host neurons in the brains of two representative murine models in which stem cell–mediated rescue of endangered neurons has been observed. Although each model features neuronal death, the insults result from different pathophysiological triggers, hence potentially informing us of the broadness of our observations across disease type.

Spinocerebellar ataxia type 1 (*SCA1*) is caused by the expansion of a polyglutamine repeat within the disease protein ataxin-1. It is characterized by ataxia due mainly to the loss of cerebellar Purkinje neurons (PNs). A transgenic mouse, *B05/+ SCA1* (12) faithfully models the human disease. PN dysfunction and ataxia are noted at 5 weeks postnatally; abnormalities in PN dendritic trees are seen at 12 weeks; and significant PN loss ensues at 24 weeks, progressing to severe reduction of molecular layer (ML) thickness and the ectopic location of the remaining PN bodies (Fig. 4*A*). When dissociated neurospheres (obtained from adult murine subventricular zone [SVZ]) were transplanted into the cerebella of *SCA1* mice at the onset of PN loss (i.e., at 24 weeks of age) and the mice were examined 2 months later, the PNs and the Purkinje cell layer (PCL) in adult *SCA1* mice (Fig. 4*C*) more closely approximated those of wild-type (WT) adult mice (Fig. 4*B*) and were significantly improved compared with those of nontransplanted, age-matched *SCA1* mice (Fig. 4*G*). This histological improvement was reflected in behavioral improvement (Fig. 4*H*) (12). In no case was this improvement accompanied by the differentiation of donor neurosphere–derived

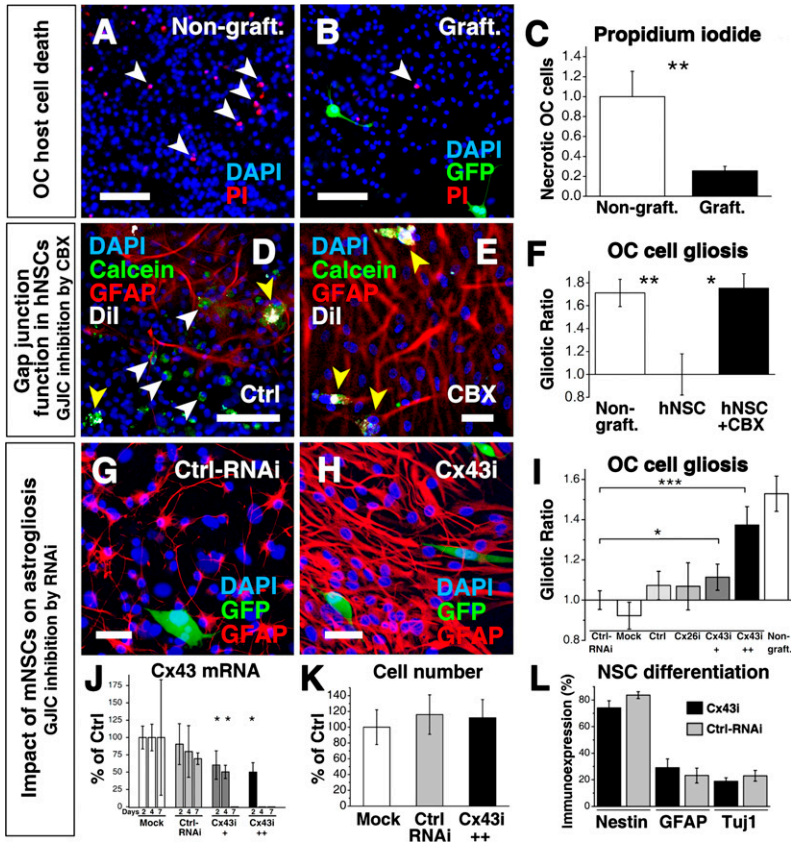

Fig. 3. Gap junctions are necessary for beneficial effect of NSCs. (*A–C*) mNSCs (GFP$^+$, green) reduce host OC cell death. The proportion of necrotic OC cells in nongrafted cultures (Nongraft.) (*A*) was decreased in grafted cultures (Graft.) (*B*) by 74% (*C*), indicated by a decrease in PI+ (red) cells (white arrowheads) in *A* and *B*. DAPI marks all nuclei blue. (*D–F*) Functional gap junction formation between hNSCs and OC cells (demonstrated transfer of calcein dye) is associated with a decrease in astrogliosis. (*D*) OC after engraftment with hNSCs, preloaded with calcein (green) and prelabeled with DiI (white). Note DiI$^+$/calcein$^+$ hNSCs (yellow arrowheads) and calcein$^+$ (green) host cells (white arrowheads). (*E* and *F*) Host astrogliosis is reduced where gap junctions have been formed by hNSCs, an action blocked by CBX. (*G*) mNSCs, including those transfected with a scrambled nonfunctional siRNA ("Ctrl-RNAi"), grafted to OCs reduce GFAP expression in OC cells at 7DIV. (*H*) Suppression of Cx43 in mNSCs by functional RNAi (Cx43i) blunted their ability to decrease OC gliosis in a dose-dependent manner, as quantified in *I:* Cx43i++ was more potent than Cx43i+. Suppression of Cx26 (Cx26i) had no impact. Control OCs (Ctrl) were grafted with mNSCs pretreated with mitomycin. In "Mock" OCs, mNSCs were exposed to the same procedures as RNAi-transfected mNSCs but without a primer being transfected. (*J*) Cx43 mRNA in mNSCs was reduced as shown at 2, 4, and 7 days posttransfection. (*K*) RNAi did not change mNSCs survival postgrafting (normalized to "Mock"; 100 ± 22%): "Ctrl-RNAi": 116 ± 25% of mock; "Cx43i": 112 ± 23% of mock. Similarly, their differentiation profile was unchanged (*L*); expression of nestin, GFAP, and Tuj1 by mNSCs transfected with Cx43i (black histograms) vs. Ctrl-RNAi (gray histograms). Only the mNSCs' antigliotic effect was abrogated: Note that the suppression of Cx43-mRNA in *J* is correlated to the mNSC effect on gliosis in *I*. $*P < 0.05$; $**P < 0.01$; $***P < 0.001$. (Bars: 100 μm, *A–D;* 20 μm, *E–H*).

cells into PNs. Rather, this near-normal PCL was populated entirely by rescued host PNs. Neurosphere-mediated PN rescue was witnessed only when direct cell contact between transplanted cells and host PNs was achieved. Indeed, we determined that rescued *SCA1* PNs were "decorated" by Cx43 expression associated with processes that extended from the transplanted neurosphere-derived cell somata, enwrapping the PN somata and contacting PN dendrites and axons (Fig. 4D_1 +D_2 and Fig. S6). This pattern of Cx43 expression indicated gap-junctional coupling between the integrated neurosphere-derived processes and the rescued endogenous PNs. Such local connexin expression was not seen in sham-transplanted age-matched adult *SCA1* PCLs (Fig. 4*E*) or in age-matched adult WT (Fig. 4*F*) but, rather, was reminiscent of the developmental profile witnessed for Cx43-mediated gap junction formation between NSCs and host cells in the OCs before electrophysiological maturity of donor-derived cells.

In the second model, the *nervous* (*nr*) mutant mouse, the same PN cell type degenerates from a different etiology and at an earlier age and more rapid pace. In addition, the murine NSCs (C17.2) were prepared entirely differently as monolayers of clonal neural progenitors in which self-renewal was enhanced. The *nr* mice, most PNs degenerate by 22–35 days of age because of a series of dysregulated intracellular signaling pathways downstream of tissue plasminogen activator (tPA) (13). mNSCs transplanted at birth into the premorbid *nr* cerebellum can rescue most PNs and their projections from impending death in early adulthood (reflected morphologically and in preserved rotarod function) if, and only if, direct cell–cell contact is made between the NSC and the PN (1). Pathologically high levels of tPA within the PN are returned to normal following transplantation of, and direct contact with, wild-type NSCs; this normal tPA level, in turn, restores equipoise to downstream intracellular pathways regulating neurotrophic factor processing and mitochondrial function (1, 13). Interestingly, gliosis and inflammation are also decreased. Because neuronal rescue in the *nr* brain paralleled that in the *SCA1* brain, and both recalled observations in the slice culture system, we again sought evidence for gap-junctional coupling between engrafted NSCs and host PNs. Indeed, in the adult cerebellar cortex of mNSC-transplanted *nr* mice, precisely in the regions where exogenous mNSCs had integrated (typically in the internal granular layer [GL]) (Fig. 5 *C* and *E*) and were interfacing with numerous rescued host PN somata (Fig. 5 *D* and *F*) (Fig. 4 in ref. 1), Cx43 immunoreactivity was abundant on rescued PN somata which, in turn, were surrounded by mNSC-derived Cx43+ cell processes (Fig. 5 *C–D*), indicative of gap-junctional coupling between the integrated mNSCs processes and the rescued endogenous PN somata, much as described above in the *SCA1* mouse. Also as in the *SCA1* mouse, the cerebellar cortices of adult wild-type mice and adult untransplanted *nr* mice evinced low or no expression of Cx43 adjacent to PN cell bodies(Fig. 5 *A* and *B*). Although some integrated mNSCs expressed Cx26 in their cell bodies, no Cx26 protein was detected in the mNSC processes or on the surface of rescued PNs (Fig. S7), consistent with our finding in vitro that Cx43 appeared earlier in the developmental profile of NSC–host neural interactions, playing a more pivotal role in host cell rescue than did Cx26.

Finally, to determine whether suppression of gap junction formation would abrogate this NSC-mediated rescue, we inhibited Cx43 action in donor mNSCs via RNAi and reassessed their impact in *nr* cerebellum (Fig. 3 *J–L,* Fig. 5 *G–J,* and Fig. S5). Although mNSCs transduced with a nonfunctional (scrambled) control RNAi ("NSCs+Ctrl-RNAi") continued to promote substantial PN rescue when grafted to organotypic cerebellar preparations from *nr* mice, mNSCs transduced with Cx43 RNAi ("NSCs+Cx43i") lost this ability, yielding PN numbers nearly as poor as in ungrafted *nr* cerebella (Fig. 5 *G–J*). The effect was dose dependent: with <30% Cx43 suppression, mNSC-mediated rescue persisted, but at 30–50% Cx43 suppression, the rescue ability of mNSCs was increasingly abrogated, and at 50–70%, suppression was optimal. Hence, Cx43

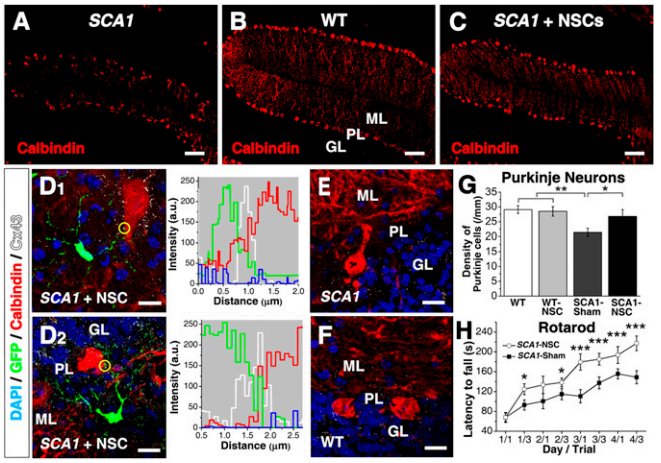

Fig. 4. Gap junction coupling between grafted mNSCs and rescued PNs in *SCA1* mice with concomitant improvement in ataxia. (*A*) Cerebellar folia of an untreated adult *SCA1* mouse (with PN loss, reduction of ML thickness, and dislocation of remaining PN somata) compared with that of age-matched WT (*B*) and *SCA1* (*C* and *D*) mice transplanted with mNSCs. In *B,* the three layers of the cerebellar cortex—molecular layer ("ML"), Purkinje layer ("PL"), and granular layer ("GL")—are shown. PNs are visualized via a calbindin antibody ("Calbindin", red). mNSC transplantation-induced *SCA1* PN number and localization are approximate normal (compare *C* with *B*). When grafted SCA1 cerebella were examined at higher magnification (D_1, D_2), "rescued" PNs were invariably in direct contact with mNSC-derived cells (GFP+, green); Cx43 (white punctuate immunoreactivity, indicative of gap junction formation) is present at these points of contact, as demonstrated when the immunofluorescence signals are analyzed quantitatively in separate channels (yellow circled region in merged images are analyzed in accompanying graphs; blue channel represents DAPI nuclear staining (Fig. S6). Of note, Cx43 is not expressed on PNs of adult sham-transplanted *SCA1* (*E*) and WT (*F*) cerebella. (*G*) Number of PNs is greater in transplanted compared with untransplanted age-matched *SCA1* mice; there is no difference in between WT and transplanted *SCA1* mice. ($n = 5$ for each condition; one-way ANOVA followed by least significant difference–Fisher posthoc test). (*H*) Transplanted *SCA1* mice remained longer on the rotarod than sham-transplanted mice (details in *SI Methods*). $^*P < 0.05$; $^{***}P < 0.001$. (Scale bars: 100 μm, *A–C;* 10 μm, *D–G.*)

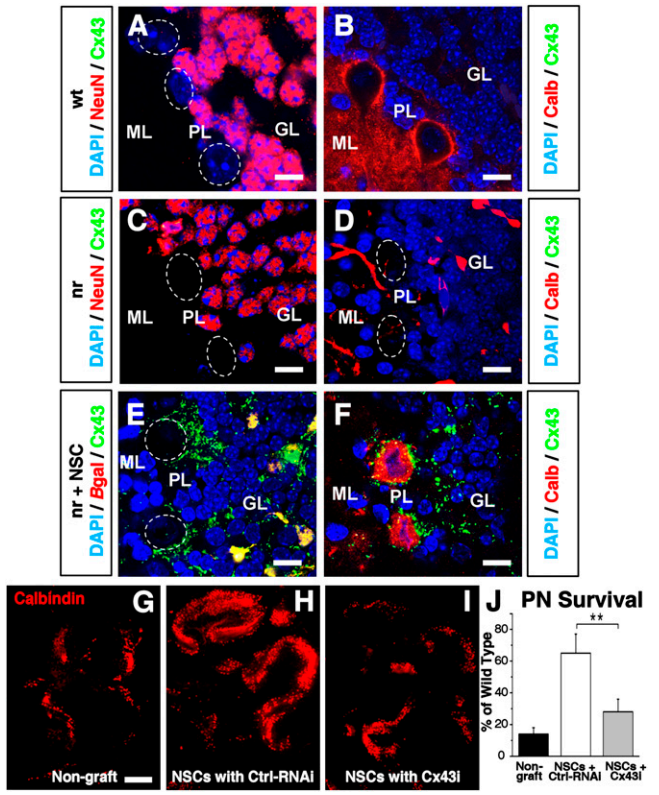

Fig. 5. Gap junction–dependent mNSC-mediated rescue of PNs in *nr* mice. The three cerebellar cortical layers (Fig. 4) are shown in three types of adult mice: ("WT"; *A* and *B*), untransplanted *nervous* ("nr"; *C* and *D*), and *nr* mice transplanted as neonates with mNSCs ("nr+NSC") (*E* and *F*). DAPI marks all nuclei blue. (*B, D,* and *F–I*) Calbindin immunoreactivity ("Calb," red) identifies PN somata in the PL and dendrites in the ML; (*A* and *C*) granule neurons (GNs) (located in the GL) are NeuN-immunoreactive (red); PNs are not (delineated by white dotted ovals). In a WT mouse (*A* and *B*), NeuN+ GNs are present in the GL (*A*) and Calb +/NeuN PNs are present in the PL (*B*). Note the absence of Cx43 (green). In an untransplanted adult *nr* mouse (*C* and *D*), Calb+ PNs are absent from the PL (*D*); NeuN+ GNs persist in the GL (*C*); the former location of degenerated PNs is indicated by dotted white circles in *C* and *D*. Again Cx43 is lacking. In adult *nr* mice transplanted as neonates with β-gal–expressing (red) mNSCs ("nr+NSC") (*E* and *F*), Calb+ rescued PNs are present in the PL (*F*) (1). Note that Cx43 (green punctate immunopositivity) is prominent on the rescued PN membrane (*F*) and on the integrated mNSC processes that surround host PN somata (*E* and *F*), and is colocalized with the βgal+ mNSC bodies (yielding orange fluorescence) (*E*). *E* presents the same field as *F* but without the Calb staining; the position of the rescued *nr* PN somata is indicated with dotted white ovals. (As in Fig. S7, Cx26-containing gap junctions are not present.) (*G–J*) Organotypic sagittal slices of cerebellum from P9 *nr* or WT mice were cultured for 7–10 days with or without grafted mNSCs. Few PNs survived in *nr* cerebella not grafted with mNSCs ("Non-graft") (*G*) compared with cerebella from WT mice (quantified in *J*). mNSCs transduced with *a* nonfunctional (scrambled) control RNAi ("NSCs+Ctrl RNAi") continued to rescue *nr* PNs. Reduction of Cx43 by RNAi in NSCs ("NSCs+Cx43i") significantly blunted the beneficial effects of NSC on *nr* PN survival ($n = 6$); PN survival in *I* was as poor as that in *G*. In *J*, host *nr* PN survival for each condition is presented as the mean percentage ± SEM of that in WT cerebella, $n = 5–6$/group. PN counts across WT cerebella varied by ≤11%. $^{**}P < 0.01$. (Scale bars: 10 μm, *A–F;* 150 μm, *G–I*).

expression in mNSCs and the gap junctions that they enable with adjacent PNs appeared to play a critical, and possibly indispensable, role in mNSC-mediated rescue of imperiled endogenous neurons.

Discussion

The critical questions posed by this study are by what mechanism exogenous NSCs (*i*) come to participate in the host nervous system's physiological properties, and (*ii*) protect host neurons from impending cell death.

Gap Junctions Mediate Early Functional Integration. Formation of functional gap junctions appears to be a very early step wherein grafted NSCs, their progeny, and host cells establish communication via Ca^{2+} even before electrophysiological maturation has been consummated (Fig. 1 *A–G* and Fig. S2). The differentiation of an NSC into a neuron during the first 4 weeks postgrafting is accompanied by a progressive decrease in resting membrane potential (consistent with an increase in Na^+/K^+ channels) (6), a decrease in R_m, and voltage-dependent spiking. However, the trains of repetitive action potentials characteristic of fully mature neurons are not yet evident by the end of that period, nor is synaptotagmin, which would indicate presence of the functional machinery for Ca^{2+}-dependent, fast synaptic vesicle exocytosis and neurotransmitter release underlying fast synaptic transmission. Similarly, strong synaptic input to the NSCs is not yet detected, a finding consistent with recent data indicating that newborn rodent neurons in vivo do not begin receiving synaptic input until 21–30 days after division, acquiring mature excitatory inputs only after 60 days (14). Nevertheless, connexin-composed gap-junctional intercellular networks, which emerge rapidly following engraftment and develop in parallel with the maturation of NSCs into neurons, appear to be sufficient to begin establishing functional cross-talk, as suggested by their influence on host Ca^{2+} waves and the downstream intercellular actions so induced. Time-lapse Ca^{2+}imaging confirms direct communication similar to that seen during normal CNS development (8, 15). Intercellular spread of synchronized $[Ca^{2+}]_i$ waves after implantation of mouse or human NSCs (Fig. 1 *A–G*, Fig. S2 *F–K* and S4 *D–F*, Movies S3, S6 and S7, and Table S2) has a speed and frequency consistent

with the establishment of functional intercellular gap junctions (15, 16) and is blocked by suppression of gap junction function. Additional evidence that the gap-junctional couplings between NSC derivatives and host cells are functional is offered by the classical defining assay for transfer of gap junction–permeable dyes, egress blocked by gap-junction antagonists (Fig. 2 *D–L* and 3 *D* and *E* and Fig. S4 *G–L*). Such functional gap junctions can be established within 2–18 h after grafting. Thus, we propose that gap-junctional intercellular networks are an early form of communication that precedes and sets the stage for later electrochemical synapses and "traditional" electrophysiological communication (17) between grafted and host cells, mimicking the connexin-mediated interaction of endogenous progenitors with their neighboring cells during CNS development.

Gap Junctions Are Essential Participants in NSC Protection of Host Neurons in Vitro and in Vivo. Exogenous NSCs can protect or rescue endogenous neurons at risk for degeneration, as first shown after spinal cord injury and established in neurodegenerative conditions in mice (13) and monkeys (2). The mechanisms underlying these events have been only partially characterized. Although diffusible factors have typically been implicated (1–3), we have begun to recognize that direct contact of NSCs with host cells is an important underappreciated feature (2, 13). In OCs, connexin-associated gap junction formation and function was pivotal for ensuring host cell well-being (Fig. 3 and Fig. S1). In vivo, NSC-mediated rescue of imperiled host neurons did not occur when gap junction formation was suppressed (Fig. 5 *G–J*). Future studies will explore how early establishment of functional gap junctions mediates rescue. It is likely that such coupling permits direct transcellular delivery of factors that promote survival and/or neutralize pathological molecules or processes. Alternatively, effective gap-junctional gating could prevent widespread passage of toxic molecules from cell-to-cell across an organ. Grafted NSCs may form gap-junctional couplings with reactive astrocytes, so that preservation of neurons could be a downstream effect of this interaction. The role of astrocytes in early stages of neuroprotection is increasingly recognized, and initial NSC-astrocyte interactions could, in addition to subsequent NSC–neuron couplings, be important especially during early stages in donor–host interactions.

That gap junction formation plays a neuroprotective role in at least two neurodegeneration models characterized by different etiologies suggests that gap junction–mediated actions might intervene at final common death pathways. That these long-lasting translationally relevant actions are not restricted solely to murine NSCs in neurogenetic diseases is suggested by preliminary findings that gap junction–associated Cx43 expression appears also to characterize the beneficial influence of human NSCs (prepared as neurospheres) on host cervical spinal motor neuronal fibers in adult rats subjected to cervical spinal cord contusion whose respiratory and motor function improves after transplantation (Fig. S8). Therefore, we are led to conjecture that such NSC-associated gap junction–mediated improvement is not limited to a particular host species and age, NSC preparation or source, region of CNS insult, or initiating pathophysiological event, and hence may have broad applicability.

Although the present study focused on Ca^{2+} signaling, other signaling molecules—such as cAMP, ATP, and Ins[1,4,5]P3 (10), as well as other ions, amino acids, and even polypeptides and microRNAs—are also gap junction permeant and may influence Na^+, Ca^{2+}, and metabolic activity, dissipate K^+ and neurotransmitter gradients, and directly control gene expression or antigen presentation (10, 11, 18). Although beyond the scope of this report, such hypotheses are now testable. (See also *SI Text*.)

In conclusion, this study suggests that one of the first, and possibly essential, ways in which grafted NSCs integrate functionally into host neural circuitry is via early functional gap-junctional coupling permitting transcellular delivery of homeostasis-modulating molecules as well as directly influencing host network coordinated activity via Ca^{2+}waves. Such actions, when recapitulated in pathological conditions, may benefit otherwise endangered neuronal populations. The molecular substrate for gap junction formation between NSCs and host cells appears to evolve in culture along a developmentally appropriate trajectory, Cx43 preceding Cx26 in the neuronal maturation of NSCs; interestingly, it is the earlier connexin, Cx43, that seems most pivotal in the NSC-mediated rescue actions.

Methods

Details of the experimental procedures and protocols are provided in *SI Text*.

For *mNSCs*, two different types of isolation, propagation and maintenance techniques were used. *i*) Neurospheres were isolated from the SVZs of 4–8 week-old FVB/N mice transgenic for GFP transcribed from a ubiquitous promoter (12). *ii*) A stable, well-characterized, clonal population of engraftable mNSCs (C17.2) was used (1, 3, 5).

"Primary" hNSCs from three different populations were assessed, all initially isolated from the telencephalic ventricular zone (VZ) of 13- or 11-week human fetal cadavers (2, 3) and *SI Text*.

Striatal and cerebellar organotypic cultures were obtained from P0–P3 and P9 rodents and cultured by the roller drum and Stoppini methods, respectively, as described in detail elsewhere (1) and in *SI Text*. Whole-cell patch-clamp recordings were performed from NSC-derived and host cells in the OCs after 7, 14, 21, and 28 DIV. $[Ca^{2+}]_i$ fluctuations were measured by time-lapse Ca^{2+} imaging in grafted and nongrafted OCs with Ca^{2+} indicator Fluo-4 and the ratiometric Ca^{2+} dye Fura-2-AM (Invitrogen) (*SI Text*). "Gliotic ratio" is the percentage of GFAP+ host cells in OCs divided by % GFAP+ host cells in grafted OCs. *SCA1* mouse and *nervous* models and experimental procedures are detailed in *SI Text* and elsewhere (5, 12). RNA interference (RNAi) for Cx26 and Cx43 (10–100 nM) and RNAi controls; scrambled siRNA, GAPHD siRNA, and nontransfected cells are detailed in *SI Text* Data are presented as mean ± SEM.

ACKNOWLEDGMENTS. We thank Ruth Detlofsson for technical assistance and Seiger and Wahlberg for providing human fetal tissue. Supported by the Swedish Research and Stockholm County Councils, KI, SSF, Freemason Child, M&M Wallenberg, Swedish Medical Association, Heart and Lung and European Science Foundations, NLM Family Fund, PALS, A-T Children's Project.

1. Li J, Imitola J, Snyder EY, Sidman RL (2006) Neural stem cells rescue nervous Purkinje neurons by restoring molecular homeostasis of tissue plasminogen activator and downstream targets. *J Neurosci* 26:7839–7848.
2. Redmond DE, Jr., et al. (2007) Behavioral improvement in a primate Parkinson's model is associated with multiple homeostatic effects of human neural stem cells. *Proc Natl Acad Sci USA* 104:12175–12180.
3. Lee JP, et al. (2007) Stem cells act through multiple mechanisms to benefit mice with neurodegenerative metabolic disease. *Nat Med* 13:439–447.
4. Gähwiler BH, Capogna M, Debanne D, McKinney RA, Thompson SM (1997) Organotypic slice cultures: A technique has come of age. *Trends Neurosci* 20:471–477.
5. Parker MA, et al. (2005) Expression profile of an operationally-defined neural stem cell clone. *Exp Neurol* 194:320–332.
6. Cai J, et al. (2004) Membrane properties of rat embryonic multipotent neural stem cells. *J Neurochem* 88:212–226.
7. Russo RE, Reali C, Radmilovich M, Fernández A, Trujillo-Cenóz O (2008) Connexin 43 delimits functional domains of neurogenic precursors in the spinal cord. *J Neurosci* 28:3298–3309.
8. Elias LA, Kriegstein AR (2008) Gap junctions: Multifaceted regulators of embryonic cortical development. *Trends Neurosci* 31:243–250.
9. Cina C, Bechberger JF, Ozog MA, Naus CC (2007) Expression of connexins in embryonic mouse neocortical development. *J Comp Neurol* 504:298–313.
10. Goodenough D, Paul DL (2009) Gap junctions. Cold Spring Harbor Perspect Biol 1(1): a002576.
11. Rouach N, Koulakoff A, Abudara V, Willecke K, Giaume C (2008) Astroglial metabolic networks sustain hippocampal synaptic transmission. *Science* 322:1551–1555.
12. Chintawar S, et al. (2009) Grafting neural precursor cells promotes functional recovery in an SCA1 mouse model. *J Neurosci* 29:13126–13135.
13. Li J, et al. (2006) Purkinje neuron degeneration in nervous (nr) mutant mice is mediated by a metabolic pathway involving excess tissue plasminogen activator. *Proc Natl Acad Sci USA* 103:7847–7852.
14. Toni N, et al. (2007) Synapse formation on neurons born in the adult hippocampus. *Nat Neurosci* 10:727–734.
15. Newman EA, Zahs KR (1997) Calcium waves in retinal glial cells. *Science* 275:844–847.
16. Weissman TA, Riquelme PA, Ivic L, Flint AC, Kriegstein AR (2004) Calcium waves propagate through radial glial cells and modulate proliferation in the developing neocortex. *Neuron* 43:647–661.
17. Benninger F, et al. (2003) Functional integration of embryonic stem cell-derived neurons in hippocampal slice cultures. *J Neurosci* 23:7075–7083.
18. Valiunas V, et al. (2005) Connexin-specific cell-to-cell transfer of short interfering RNA by gap junctions. *J Physiol* 568:459–468.